ADVANCED OPTICAL MATERIALS
www.advopticalmat.de

ZnO p–n Homojunction Random Laser Diode Based on Nitrogen-Doped p-type Nanowires

*Jian Huang, Sheng Chu, Jieying Kong, Long Zhang, Casey M. Schwarz, Guoping Wang, Leonid Chernyak, Zhanghai Chen, and Jianlin Liu**

An electrically pumped ZnO homojunction random laser diode based on nitrogen-doped p-type ZnO nanowires is reported. Nitrogen-doped ZnO nanowires are grown on a ZnO thin film on a silicon substrate by chemical vapor deposition without using any metal catalyst. The p-type behavior is studied by output characteristics and transfer characteristic of the nanowire back-gated field-effect transistor, as well as low-temperature photoluminescence. The formation of the p–n junction is confirmed by the current–voltage characteristic and electron beam-induced current. The nanowire/thin-film p–n junction acts as random laser diode. The random lasing behavior is demonstrated by using both optical pumping and electrical pumping, with thresholds of 300 kW/cm^2 and 40 mA, respectively. The angle-dependant electroluminescence of the device further proves the random lasing mechanism. An output power of 70 nW is measured at a drive current of 70 mA.

1. Introduction

Random lasers, which are based on highly disordered gain medium, have attracted much attention owing to their various potential applications. For example, random lasers are ideal for display applications because they usually exhibit a very broad angular distribution.[1] Besides, they can be used for remote heat sensing,[2] document encoding,[3] chemical sensing,[4] and even medical diagnostics.[5,6] Furthermore, compared with conventional lasers, the unique advantage of random lasers lies in simple structures, which can be realized by cost-effective processing techniques with various materials. The random laser action has been observed in many different structures including nanoparticles,[7,8] nanowires[9–11] and thin films,[12] and in different materials such as ZnO,[12,13] liquid dye[14] and solid state polymer.[15]

Among various materials for random lasing, ZnO is a promising material owing to its direct band gap and large exciton binding energy of ~60 meV at room temperature.[16] Its one dimensional structure, which can be synthesized by various low-cost methods, is an excellent optical cavity for random lasers. Many attempts have been made to induce lasing behavior in ZnO nanowire-based devices.[17–24] Nevertheless, most of the random lasers based on ZnO nanowires are induced by optical pumping.[17–20] For practical laser applications, electrical pumping is needed. Electrically pumped ZnO nanowires random lasers have been demonstrated based on ZnO metal insulator semiconductor structures[21,22] and heterojunctions,[23,24] while the nanowires random laser diode based on ZnO p–n homojunction, which can significantly enhance the output power for practical applications, has not been reported yet. The difficulty mainly lies in the problem of p-type doping of ZnO nanowires.

Nitrogen has been reported to be a good p-type dopant for ZnO thin film,[25–27] although Lyons et al. also predicted that nitrogen doping may not produce p-type ZnO at all.[28] In order to clarify this controversial research topic, tremendous experimental and theoretical studies from many research groups may be necessary. Recently, Yuan et al. reported CVD growth of nitrogen-doped p-type ZnO nanowires.[29] The nanowires were grown on sapphire substrate by using gold as catalyst. Gold can help the growth of ZnO nanowires, however it may be an p-type dopant or deep-level impurity[30] as the atoms are inadvertently introduced into the nanowires during the growth,[31] which complicates the origin of the p-type conductivity. In this research, we grew nitrogen-doped p-type ZnO nanowires without metal catalyst on ZnO thin film and formed the p–n homojunction. Based on this structure, we demonstrated electrically pumped ZnO nanowires homojunction random laser device. These results suggest that nitrogen can be an effective p-type dopant for ZnO nanowires.

J. Huang,[+] Dr. S. Chu,[+] J. Kong, Dr. G. Wang, Prof. J. Liu
Quantum Structures Laboratory
Department of Electrical Engineering
University of California at Riverside
Riverside, CA, 92521, USA
E-mail: jianlin@ee.ucr.edu
L. Zhang, Prof. Z. Chen
Laboratory of Advanced Materials
Department of Physics
Fudan University
Shanghai, 200433, China
C. M. Schwarz, Prof. L. Chernyak
Department of Physics
University of Central Florida
Orlando, FL, 32816, USA
[+] These authors contributed equally to this work.

DOI: 10.1002/adom.201200062

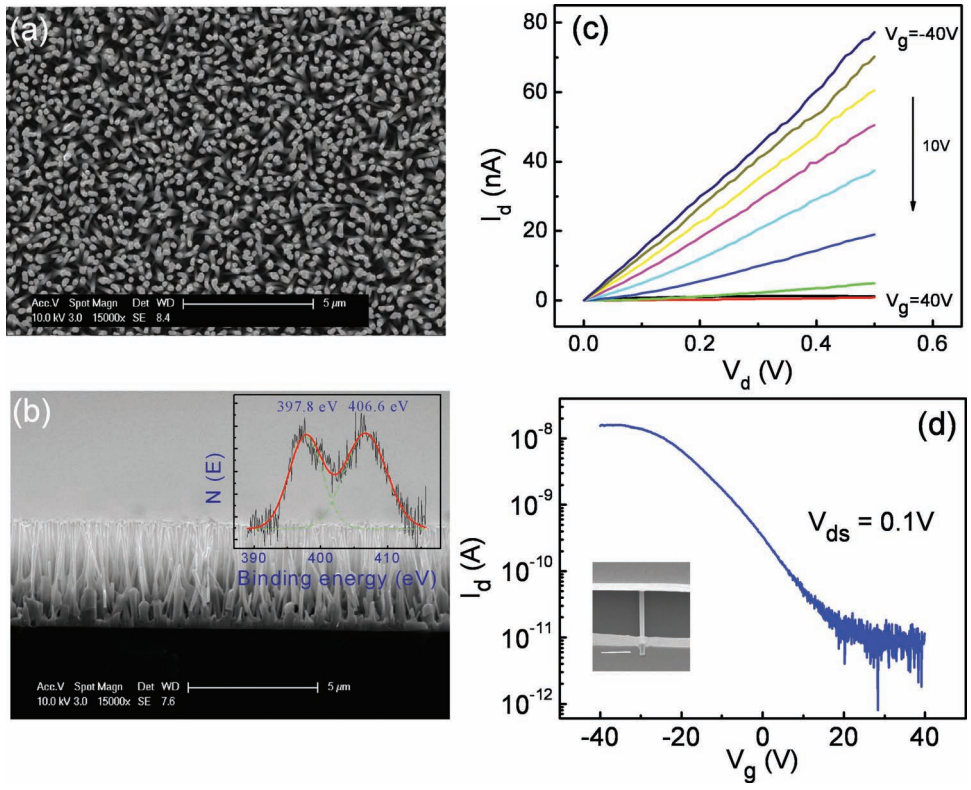

Figure 1. (a) Top view SEM image of nitrogen-doped ZnO nanowires. The sidewall of the nanowires can be seen, indicating that the nanowires are not totally vertically aligned. (b) Side view SEM image of nitrogen-doped ZnO nanowires. Inset: XPS spectrum of the sample. (c) I_d-V_d curves of nitrogen-doped ZnO nanowire back-gated FET. V_g increases from –40 V to 40 V with a 10 V step. (d) I_d-V_g curve of nitrogen-doped nanowire back-gated FET. Inset: SEM image of the measured FET device. The scale bar is 2 μm.

2. Results and Discussion

Figure 1a and b show scanning electron microscope (SEM) images of the top view and cross sectional view of the nanowires sample, respectively. The average diameter of the nanowires is about 200 nm and the length is about 3.5 μm. From the cross sectional view of the nanowires (Figure 1b), it is noticeable that most nanowires are not vertically aligned, but tilted 10–15 degrees with respect to the normal of the substrate surface. This may be due to the rough surface of the original ZnO thin film seed.

X-ray photoelectron spectroscopy (XPS) result of nitrogen-doped ZnO nanowires is shown in the inset of Figure 1b. Two N 1s related peaks at 397.8 eV and 406.6 eV are evident. Both peaks have been reported in the p-type nitrogen-doped ZnO thin film.[32] The low energy peak at 397.8 eV corresponds to nitrogen substitution on the oxygen site,[33] which is the desired process for p-type doping. The peak at 406.6 eV is assigned to be the N 1s binding energy of NO_3^- radical.[33,34] This high-energy peak, which is commonly observed in the oxygen rich compound,[33] suggests that these nanowires were grown under an oxygen rich condition.[34] The oxygen rich growth condition can suppress the "intrinsic" donors such as zinc interstitials and oxygen vacancies[35,36] and help achieve p-type conductivity. From the XPS result, the approximate atomic concentration of nitrogen is 0.1%.

To study the electrical transport properties of nanowires, a single nanowire back-gated field effect transistor (FET) was fabricated. Figure 1c shows I_d-V_d curves of the FET (an SEM image of the device is shown as an inset in Figure 1d). It is clear that all I_d-V_d curves are linear, indicating that Ohmic contacts have been formed between the nitrogen doped ZnO nanowire and Ni/Au electrodes. The I_d-V_d curves show clear field effect characteristic of p-type conductivity: as the gate voltage increases, the conductance of the nanowire decreases. Figure 1d shows transfer characteristic (I_d-V_g) of the device. The curve with an on/off ratio over 100 represents the typical curve for good p-type conductivity in ZnO nanowire. The hole concentration can be calculated by using the equation:[37] $p_0 = \left(\frac{V_{th}}{q}\right)\left(\frac{4}{\pi d^2}\right)\left[\frac{2\pi\varepsilon_0\varepsilon_r}{\ln(4h/d)}\right]$, where ε_0, ε_r, h, d, V_{th} are the dielectric constant in vacuum, dielectric constant of SiO_2 (3.9), thickness of the SiO_2 (300 nm), diameter of the nanowire (200 nm) and threshold voltage of the FET (about 20 V from the I_d-V_g curve), respectively. The hole concentration of the nanowire is calculated to be about 3×10^{17} cm^{-3}. The hole mobility can be estimated by $\mu_m = g_m\left(\frac{L}{V_d}\right)\left[\frac{\ln(4h/d)}{2\pi\varepsilon_0\varepsilon_r}\right]$[37] where g_m is the transconductance and L is the effective length of the nanowire (~3 μm). The mobility is then calculated to be around 1.5 $cm^2/(V_s)$.

The acceptor activation energy is one of the most important parameters to evaluate the p-type dopant in semiconductors and can be extracted by temperature-dependent PL spectra. The p-type characteristic of the nitrogen-doped ZnO nanowires in

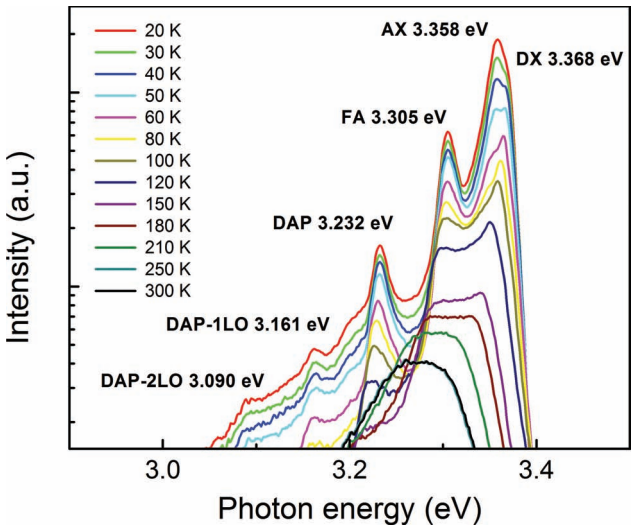

Figure 2. Temperature dependent PL spectra of nitrogen-doped ZnO nanowires. The temperature ranges from 20 K to 300 K.

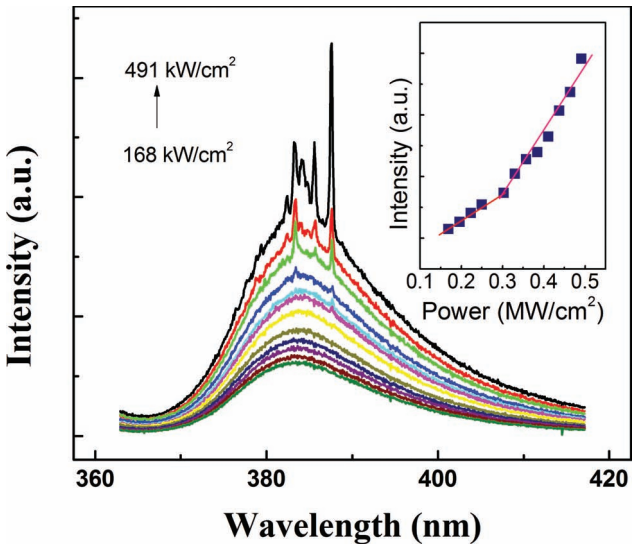

Figure 3. Room-temperature optically pumped lasing spectra. Inset: integrated spectra intensity as a function of pumping power density. Solid lines are guide to the eye, indicating threshold power P_{th} (0.3 MW/cm^2).

PL is summarized in **Figure 2**. An He-Cd laser with an excitation wavelength of 325 nm was used in this experiment. The acceptor bound exciton (*AX*) and donor bound exciton (*DX*) peaks are at 3.358 eV and 3.368 eV, respectively. The acceptor activation energy ΔE_A for the N(O) acceptor could be derived from the binding energy between the acceptor and free exciton by using Hayne's rule.[38] ΔE_A is calculated to be 198 meV by using the binding energy between the acceptor and free exciton (19.8 meV) from the fitting of the temperature-dependent PL spectra (Supporting Information). The peaks at around 3.305 eV and 3.232 eV are due to free electron to acceptor (*FA*) emission and donor-acceptor-pair (*DAP*) emission (Supporting Information), respectively.[39,40] The longitudinal-optical (*LO*) phonon replicas of the *DAP* emission are shifted by the ZnO phonon energy of ~71 meV. The activation energy of an acceptor ΔE_A can be calculated with the equation[41] $\Delta E_A = E_{gap} - E_{DAP} - \Delta E_D + < \frac{e^2}{4\pi\varepsilon_0\varepsilon_{ZnO} r_{DAP}} >$. The donor binding energy ΔE_D is reported to be about 30 meV[42–44] and the intrinsic band gap $E_{gap} = 3.435\,eV$ at 20 K.[44] ε_{ZnO} is the dielectric constant of ZnO (8.6). r_{DAP} is the average donor-acceptor pair distance. The last term represents the Coulomb interaction between the donors and acceptors and the value is around 20 meV.[41,45] Based on the assignment of the 3.232 eV peak as the *DAP* transition energy, the acceptor activation energy ΔE_A for the N(O) acceptor is 195 meV.

In order to get more insight on nitrogen acceptor in the p-type ZnO nanowires, the

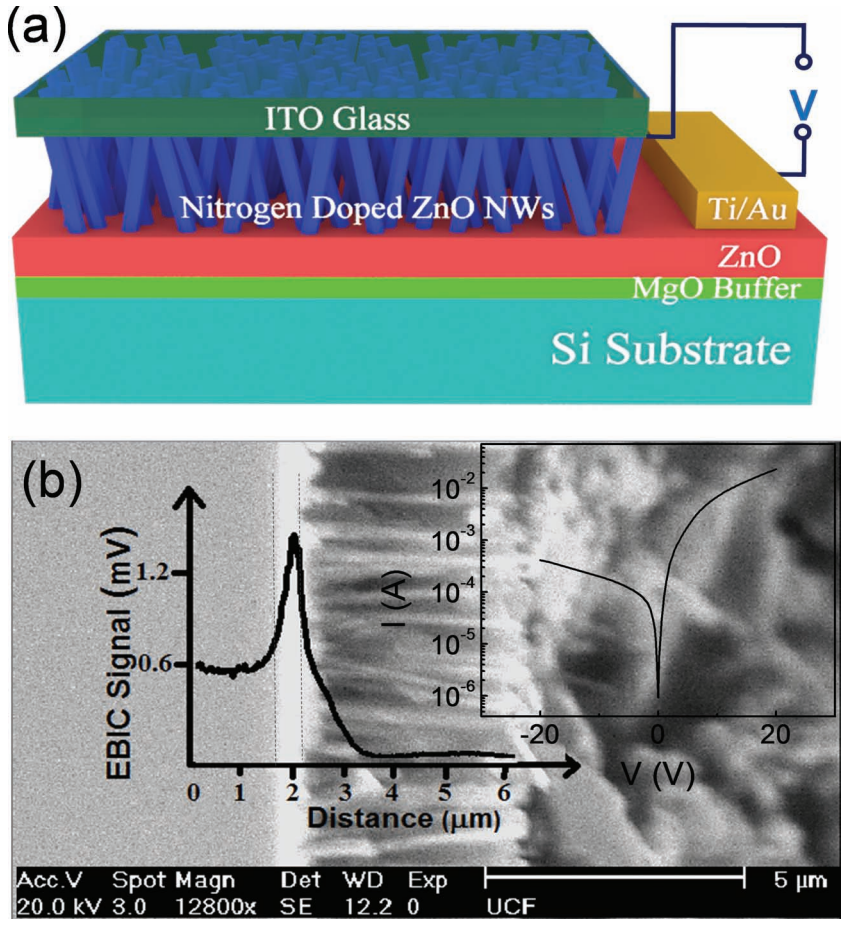

Figure 4. (a) Schematic of the electrically pumped laser device. (b) EBIC profile superimposed on the side-view SEM image of the cleaved device. Inset: *I-V* characteristic of the ITO/ZnO nanowires/ZnO thin film/Ti/Au random laser device. The Ti/Au contact is grounded.

acceptor activation energy can also be evaluated based on the carrier density approach. From the semiconductor physics, the hole concentration can be calculated by:

$$p_0 = 2\frac{(2\pi m_p^* k_B T)^{3/2}}{h^3} e^{-(E_F - E_v)/k_B T} \quad (1)$$

where m_p^* is the effective hole mass ~$0.6m_0$.[46] The occupation probability for acceptor can be described by the Fermi function: $f_A(E) = \frac{1}{\frac{1}{2}e^{(E_F - E_A)/k_B T}+1}$, where E_A is the acceptor energy. In the undoped ZnO nanowires sample, the electron concentration is on the order of 10^{17} cm^{-3} (Supporting Information), therefore we can reasonably assume a background electron carrier concentration to be between 1×10^{17} cm^{-3} and 1×10^{18} cm^{-3} for calculation. Considering the compensation effect, the activated acceptor concentration ranges from 4×10^{17} cm^{-3} to 1.3×10^{18} cm^{-3}. The atom density of ZnO is 8.28×10^{22} cm^{-3} and the nitrogen atomic ratio is 0.1% from the XPS result. So about 0.5%~1.7% of acceptors are activated, which means $f_A(E)$ ranges from 0.995 to 0.983. From the Fermi function, the Fermi energy is $E_F = k_B T \ln\frac{2(1-f_A(E))}{f_A(E)} + E_A$. Inserting the Fermi energy into Equation (1), and taking T = 300 K, the activation energy $\Delta E_A = E_A - E_v$ is between 215 and 183 meV, which is in good agreement with the results from PL.

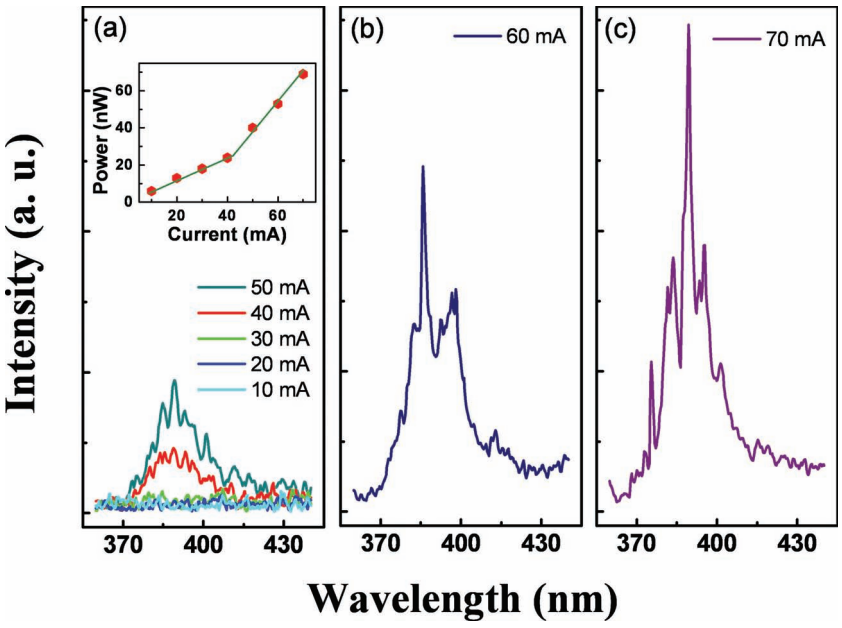

Figure 5. Lasing characterization of the device by electrical pumping. EL spectra of the laser device operated at the drive current from (a) 10 mA to 50 mA, (b) 60 mA and (c) 70 mA. Inset of (a) is the output power as a function of drive current.

Figure 3 shows the evolution of PL emission spectra of the ZnO nanowires as a function of excitation pumping power at room-temperature. The excitation source in this experiment is a Nd:YAG pulse laser with an output wavelength of 355 nm. The laser has 10 Hz frequency and 3 ns pulse duration. A silicon CCD is used as the detector and the spectrum resolution is 0.054 nm. The pumping power ranges from 168 kW/cm^2 to 491 kW/cm^2 with average steps of 30 kW/cm^2. Lasing characteristics are evident from the spectra and the threshold power is found to be at around 300 kW/cm^2 (Figure 3 inset). Below the threshold only a single broad spontaneous emission peak is observed. When the pumping power reaches the threshold, a few discrete narrow lasing peaks with linewidth of about 0.4 nm emerge from the single broad spontaneous emission spectrum. At higher pumping powers, more peaks also begin to emerge because more lasing modes are activated. These peaks are not evenly spaced and are not stable, which suggest that the lasing shall originate from random lasing based on the multiple light scattering among the nanowires rather than Fabry-Perot mechanism, where each nanowire serves as gain cavity.[47] The density of electron-hole pairs (n_p) produced by the optical pumping can be calculated by $n_p = I_{exc}\tau / h\omega l$.[48] Here, I_{exc} is the excitation power, τ is the spontaneous emission lifetime (about 300 ps for ZnO)[49] and l is the diffusion length (about 2 μm for ZnO).[50] At the threshold pumping power 300 kW/cm^2, n_p is calculated to be 8.5×10^{17} cm^{-3}. Because Mott density in ZnO has been controversial as seen in between 5×10^{17} cm^{-3} and 3.7×10^{19} cm^{-3},[48,51,52] the gain may originate from exciton interaction, or from electron hole plasma, or from both.

Figure 4a shows the schematic of the electrical pumping device. The fabrication of the device is described in the method section. The formation of the ZnO homojunction between the nanowires and thin film was investigated by electron-beam-induced current (EBIC) profiling, which was widely used to investigate the junctions in semiconductors.[53,54] Figure 4b shows EBIC profile superimposed on a cross-sectional SEM image. An accelerating voltage of 30 kV was applied, corresponding to the electron penetration depth of 1.5 μm. The EBIC signal forms a clear peak on the ZnO thin film/nanowire junction due to electron-hole pairs from electron beam irradiation generation drifted by built-in electric field in the p–n junction depletion region. The inset of Figure 4b shows current-voltage (*I-V*) characteristic of the ZnO p–n junction. Rectifying behavior is clearly observed. Both *I-V* and EBIC results indicate the formation of ZnO nanowire/ZnO thin film p–n homojunction.

Figure 5a–c show electroluminescence (EL) spectra of the device with the increase of drive current. The detector was placed perpendicular to the sample surface. As can be seen from Figure 5a, for the current below 40 mA, the EL emission is relatively weak and the spectrum is greatly spoiled by noise. At 40 mA, a single broad spontaneous emission peak centered at around 388 nm appears, which is ascribed to the near band edge UV emission from ZnO. As the current increases further (50 mA), a few randomly distributed narrow peaks appear in the spectrum. The lasing peaks become stronger and sharper and more peaks show up as the current reaches 60 mA (Figure 5b) and 70 mA (Figure 5c). The linewidth of these peaks is less than 2 nm. The detected output power as a function of injection current is shown in the inset of Figure 5a. The output power was measured using a Thorlabs PM100 Optical Power Meter. The solid lines are the guide to the eye, showing the threshold

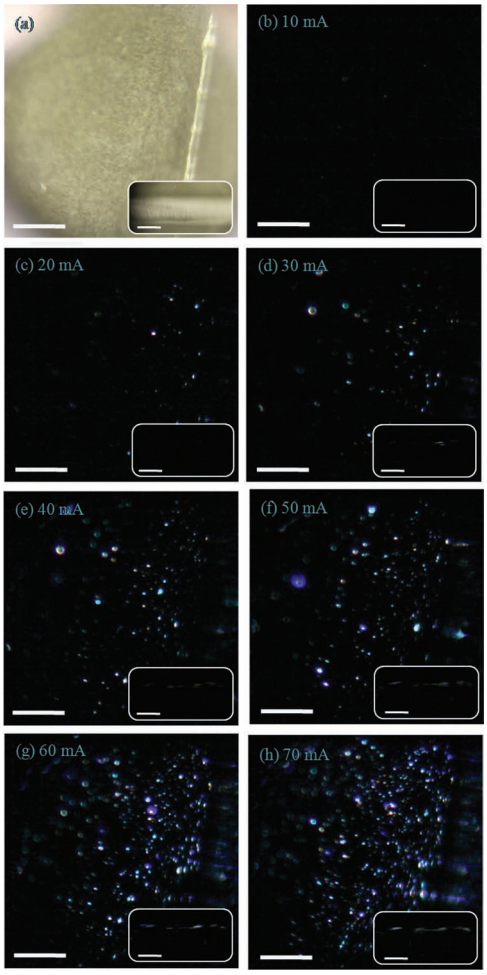

Figure 6. Optical microscope images of the lasing device with different drive current. The first image was taken with lamp illumination and zero current injection. The inset of each image is the corresponding side-view microscope image of the device. All the scale bars are 300 µm.

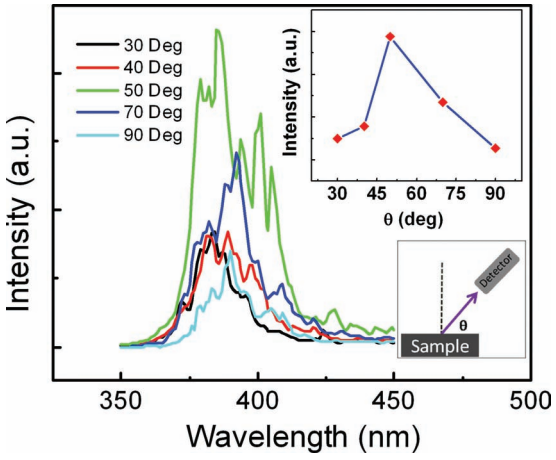

Figure 7. Angle-dependent EL of the device. Top inset is the integrated spectra intensity as a function of angle. Bottom inset shows the schematic of measurement setup. θ is the angle between the sample surface and detector.

current of ~40 mA. This is consistent with the results from the integrated intensity of the spectra (Supporting Information). The output power is about 70 nW at 70 mA drive current. The detector cannot receive all the light from the device, and just part of the power has been detected, leading to this relatively low output power. However, this value is already over one order of magnitude higher than that of the metal oxide semiconductor random laser structure reported.[21] As seen from the EL spectra, the spacing between the adjacent sharp peaks is not uniform and the peak positions between different measurements are different. Therefore, the lasing peaks in the EL spectra should be related to the random lasing instead of F-P lasing. These multiple sharp peaks in the spectra between 370 nm and 410 nm represent different lasing modes of the nanowires. The far field microscope top view images and side view images (inset) of the laser at different injection current were taken by the commercial digital camera (**Figure 6**). Randomly distributed bright spots can be seen from the top view images. As the drive current increases, more bright emission spots are observed and the luminance becomes higher and higher.

Figure 7 shows lasing emission spectra at different observation angles. The injection current is the same for all spectra at 70 mA. The bottom inset in Figure 7 is a schematic of the measurement setup. The θ is defined as the observation angle between the detector and sample surface. As shown in Figure 7, the laser emission spectra varied drastically with the observation angle. The spectra from different angles show different lasing peaks and different intensities. This is because for a random laser, different random cavities emit the lasing signals in different directions, and the detector placed at a certain angle can only collect the laser signals along its corresponding direction. The top inset in Figure 7 shows the integrated spectra intensity versus angle θ. The intensity has a broad distribution and the maximum intensity shows up at $\theta = 50$ degrees. Because the nanowires are not totally vertically aligned, the top facets of the nanowires are not in parallel with the interface between ZnO and silicon substrate. Thus, F-P cavity cannot be formed and the lasing signals should originate from the random scattering among the ZnO nanowire arrays. The non-homogeneity in the lasing emission profile, which has been reported in nanopowders and nanowires,[55,56] should be induced by the random tilted angle of the nanowires in our sample.

3. Conclusion

In summary, p-type nitrogen-doped ZnO nanowires were grown by using CVD without any metal catalyst on ZnO seed layer on silicon substrate. The p-type behavior was studied by the output characteristic and transfer characteristic of the nanowire back-gated FET and PL. An acceptor activation energy of ~200 meV was obtained from PL and carrier concentration statistics. The formation of the p–n junction was confirmed by *I-V* and EBIC results. The lasing behaviors were studied by using both optical pumping and electrical pumping. Above the threshold pumping power/current, random lasing actions featuring a series of lasing peaks in the spectra were observed. The output power of the electrically pumped laser was measured to

be 70 nW at a drive current of 70 mA. The angle dependant EL result shows that the emission has a broad angle distribution, further indicating the formation of ZnO nanowires p–n homojunction random laser.

4. Experimental Section

Nanowire Growth: Nitrogen-doped ZnO nanowires were grown in a CVD furnace on a high-quality undoped ZnO seed layer on n-type Si (100) substrate. The 400 nm n-type seed layer was grown on a 3-nm MgO buffer in plasma-assisted molecular beam epitaxy (MBE) (Supporting Information). To grow nitrogen-doped p-type ZnO nanowires, argon diluted oxygen (0.5%) was used as reaction gas and argon diluted N_2O (0.5%) was used as dopant gas. The flow rates were 200 sccm and 50 sccm, respectively. A flow of 1000 sccm nitrogen was passed continuously through the furnace during the growth. Zinc powder (99.999% Sigma Aldrich) was placed in a silica bottle and served as source material. The substrate was positioned at the center of the silica tube, which was about 1 cm away from the silica bottle at the downstream side. The growth temperature is 650 °C and the growth duration is 40 min. Part of the substrate was covered by a piece of silicon wafer during the growth for subsequent electrical contact formation on the ZnO film.

Nanowire/Thin Film Laser Diode Fabrication: The ITO glass was clamped on the top end of the nanowires as the top electrode and Ti/Au (10 nm/100 nm) was deposited on the undoped n-type ZnO as the ground electrode using e-beam evaporation. During the Ti/Au metal evaporation, the nanowires were protected by an aluminium foil.

Nanowire Back-Gated FET Fabrication: The nitrogen-doped ZnO nanowires were transferred onto a SiO_2 (300 nm)/p+-Si wafer and then the Ni/Au electrodes were formed on an individual nanowire by using photolithography and e-beam evaporation. Al was deposited on the back of the silicon wafer to form the back gate electrode.

Supporting Information

Supporting Information is available from the Wiley Online Library or from the author.

Acknowledgments

The authors would like to thank the National Science Foundation (grant No. ECCS 0900978) for ZnO device work and the Department of Energy (DE-FG02-08ER46520) for p-type ZnO research.

Received: December 16, 2012
Revised: January 8, 2013

[1] D. S. Wiersma, *Nat. Physics* **2008**, *4*, 359–367.
[2] D. S. Wiersma, S. Cavalieri, *Nature* **2001**, *414*, 708.
[3] R. M. Balachandran, D. P. Pacheco, N. M. Lawandy, *Appl. Opt.* **1996**, *35*, 640–643.
[4] Q. Song, S. Xiao, Z. Xu, V. M. Shalaev, Y. L. Kim, *Opt. Lett.* **2010**, *35*, 2624–2626.
[5] R. C. Polson, Z. V. Vardeny, *Appl. Phys. Lett.* **2004**, *85*, 1289–1291.
[6] Q. Song, Z. Xu, S. H. Choi, X. Sun, S. Xiao, O. Akkus, Y. L. Kim, *Biomed. Opt. Express* **2010**, *1*, 1401–1407.
[7] S. García-Revilla, M. Zayac, R. Balda, M. Al-Saleh, D. Levy, J. Fernández, *Opt. Express* **2009**, *17*, 13202–13215.
[8] X. Meng, K. Fujita, S. Murai, T. Matoba, K. Tanaka, *Nano Lett.* **2011**, *11*, 1374–1378.
[9] V. V. Zalamai, V. V. Ursaki, C. Klingshirn, H. Kalt, G. A. Emelchenko, A. N. Redkin, *Appl. Phys. B: Lasers Opt.* **2009**, *97*, 817–823.
[10] M. L. Lu, H. Y. Lin, T. T. Chen, Y. F. Chen, *Appl. Phys. Lett.* **2011**, *99*, 091106.
[11] R. Chen, M. I. B. Utama, Z. P. Peng, B. Peng, Q. H. Xiong, H. D. Sun, *Adv. Mater.* **2011**, *23*, 1404–1408.
[12] S. Chu, M. Olmedo, Z. Yang, J. Kong, J. Liu, *Appl. Phys. Lett.* **2008**, *93*, 181106.
[13] H. K. Liang, S. F. Yu, H. Y. Yang, *Appl. Phys. Lett.* **2010**, *97*, 241107.
[14] D. S. Wiersma, S. Cavalieri, *Phys. Rev. E* **2002**, *66*, 056612.
[15] T. Zhai, X. Zhang, Z. Pang, X. Su, H. Liu, S. Feng, L. Wang, *Nano Lett.* **2011**, *11*, 4295–4298.
[16] E. O. Kane, *Phys. Rev. B* **1978**, *18*, 6849.
[17] H. C. Hsu, C. Y. Wu, W. F. Hsieh, *J. Appl. Phys.* **2005**, *97*, 064315.
[18] H. Y. Yang, S. F. Yu, H. K. Liang, C. Pang, B. Yan, T. Yu, *J. Appl. Phys.* **2009**, *106*, 043102.
[19] J. Fallert, R. J. B. Dietz, M. Hauser, F. Stelzl, C. Klingshirn, H. Kalt, *J. Lumin.* **2009**, *129*, 1685–1688.
[20] Y. Chen, Y. Chen, *Opt. Express* **2011**, *19*, 8728–8734.
[21] X. Ma, J. Pan, P. Chen, D. Li, H. Zhang, Y. Yang, D. Yang, *Opt. Express* **2009**, *17*, 14426.
[22] X. Y. Liu, C. X. Shan, S. P. Wang, Z. Z. Zhang, D. Z. Shen, *Nanoscale* **2012**, *4*, 2843–2846.
[23] K. Kim, T. Moon, J. Kim, S. Kim, *Nanotechnology* **2011**, *22*, 245203.
[24] J. Y. Zhang, Q. F. Zhang, T. S. Deng, J. L. Wu, *Appl. Phys. Lett.* **2009**, *95*, 211107.
[25] A. Tsukazaki, A. Ohtomo, T. Onuma, M. Ohtani, T. Makino, M. Sumiya, K. Ohtani, S. F. Chichibu, S. Fuke, Y. Segawa, H. Ohno, H. Koinuma, M. Kawasaki, *Nat. Mater.* **2005**, *4*, 42–46.
[26] D. C. Look, D. C. Reynolds, C. W. Litton, R. L. Jones, D. B. Eason, G. Cantwell, *Appl. Phys. Lett.* **2002**, *81*, 1830–1832.
[27] C. C. Lin, S. Y. Chen, S. Y. Cheng, H. Y. Lee, *Appl. Phys. Lett.* **2004**, *84*, 5040.
[28] J. L. Lyons, A. Janotti, C. G. Van de Walle, *Appl. Phys. Lett.* **2009**, *95*, 252105.
[29] G. D. Yuan, W. J. Zhang, J. S. Jie, X. Fan, J. A. Zapien, Y. H. Leung, L. B. Luo, P. F. Wang, C. S. Lee, S. T. Lee, *Nano Lett.* **2008**, *8*, 2591–2597.
[30] Y. Yan, M. M. Al-Jassim, S. H. Wei, *Appl. Phys. Lett.* **2006**, *89*, 181912.
[31] J. S. Lee, M. S. Islam, S. Kim, *Nano Lett.* **2006**, *6*, 1487–1490.
[32] M. Joseph, H. Tabata, T. Kawai, *Jpn. J. Appl. Phys.* **1999**, *38*, L1205–L1207.
[33] C. L. Perkins, S. H. Lee, X. Li, S. E. Asher, T. J. Coutts, *J. Appl. Phys.* **2005**, *97*, 034907.
[34] J. Torres, C. C. Perry, S. J. Bransfield, D. H. Fairbrother, *J. Phys. Chem. B* **2003**, *107*, 5558–5567.
[35] D. C. Look, J. W. Hemsky, J. R. Rizelove, *Phys. Rev. Lett.* **1999**, *82*, 2552.
[36] S. B. Zhang, S. H. Wei, A. Zunger, *Phys. Rev. B* **2001**, *63*, 075205.
[37] G. Wang, S. Chu, N. Zhan, Y. Lin, L. Chernyak, J. Liu, *Appl. Phys. Lett.* **2011**, *98*, 041107.
[38] F. X. Xiu, Z. Yang, L. J. Mandalapu, D. T. Zhao, J. L. Liu, *Appl. Phys. Lett.* **2005**, *87*, 252102.
[39] F. Reuss, C. Kirchner, T. Gruber, R. Kling, S. Maschek, W. Limmer, A. Waag, P. Ziemann, *J. Appl. Phys.* **2004**, *95*, 3385.
[40] S. Karamat, R. S Rawat, T. L. Tan, P. Lee, S. V. Springham, E. Ghareshabani, R. Chen, H. D. Sun, *Appl. Surf. Sci.* **2011**, *257*, 1979–1985.
[41] D. C. Look, B. Claflin, *Phys. Stat. Sol. B* **2004**, *241*, 624–630.
[42] D. C. Look, G. C. Farlow, P. Reunchan, S. Limpijumnong, S. B. Zhang, K. Nordlund, *Phys. Rev. Lett.* **2005**, *95*, 225502.

[43] V. Avrutin, D. J. Silversmith, H. Morkoc, *Proc. IEEE* **2010**, *98*, 1302–1315.
[44] B. K. Meyer, H. Alves, D. M. Hofmann, W. Kriegseis, D. Forster, F. Bertram, J. Christen, A. Hoffmann, M. Straßburg, M. Dworzak, U. Haboeck, A. V. Rodina, *Phys. Stat. Sol. B* **2004**, *241*, 231–260.
[45] A. Zeuner, H. Alves, D. M. Hofmann, B. K. Meyer, A. Hoffmann, U. Haboeck, M. Strassburg, M. Dworzak, *Phys. Stat. Sol. B* **2002**, *234*, R7–R9.
[46] N. N. Syrbu, I. M. Tiginyanu, V. V. Zalamai, V. V. Ursaki, E. V. Rusu, *Physica B* **2004**, *353*, 111–115.
[47] S. Chu, G. Wang, W. Zhou, Y. Lin, L. Chernyak, J. Zhao, J. Kong, L. Li, J. Ren, J. Liu, *Nat. Nanotechnol.* **2011**, *6*, 506.
[48] C. Klingshirn, R. Hauschild, J. Fallert, H. Kalt, *Phys. Rev. B* **2007**, *75*, 115203.
[49] D. C. Reynolds, D. C. Look, B. Jogai, J. E. Hoelscher, R. E. Sherriff, M. T. Harris, M. J. Callahan, *J. Appl. Phys.* **2000**, *88*, 2152–2153.
[50] O. Lopatiuk-Tirpak, L. Chernyak, F. X. Xiu, J. L. Liu, S. Jang, F. Ren, S. J. Pearton, K. Gartsman, Y. Feldman, A. Osinsky, P. Chow, *J. Appl. Phys.* **2006**, *100*, 086101.
[51] M. A. M. Versteegh, T. Kuis, H. T. C. Stoof, J. I. Dijkhuis, *Phys. Rev. B* **2011**, *84*, 035207.
[52] Y. Chen, N. T. Tuan, Y. Segawa, H. J. Ko, S. K. Hong, T. Yao, *Appl. Phys. Lett.* **2001**, *78*, 1469.
[53] S. Hoffmann, J. Bauer, C. Ronning, Th. Stelzner, J. Michler, C. Ballif, V. Sivakov, S. H. Christiansen, *Nano Lett.* **2009**, *9*, 1341.
[54] O. Lopatiuk-Tirpak, L. Chernyak, L. Mandalapu, Z. Yang, J. L. Liu, K. Gartsman, Y. Feldman, Z. Dashvsky, *Appl. Phys. Lett.* **2006**, *89*, 142114.
[55] H. Cao, Y. G. Zhao, H. C. Ong, R. P. H. Chang, *Phys. Rev. B* **1999**, *59*, 15107–15111.
[56] M. A. Zimmler, F. Capasso, S. Muller, C. Ronning, *Semicond. Sci. Technol.* **2010**, *25*, 024001.